JACS
JOURNAL OF THE AMERICAN CHEMICAL SOCIETY
Communication
pubs.acs.org/JACS

Spatial Organization of Lipid Phases in Micropatterned Polymer-Supported Membranes

Friedrich Roder, Oliver Birkholz, Oliver Beutel, Dirk Paterok, and Jacob Piehler*

Division of Biophysics, Department of Biology, University of Osnabrück, 49069 Osnabrück, Germany

Supporting Information

ABSTRACT: We have established an approach for the spatial control of lipid phase separation in tethered polymer-supported membranes (PSMs), which were obtained by vesicle fusion on a poly(ethylene glycol) polymer brush functionalized with fatty acid moieties. Phase separation of ternary lipid mixtures (1,2-dioleoyl-*sn*-glycero-3-phosphocholine/sphingomyelin/cholesterol) into liquid-disordered (l_d) and liquid-ordered (l_o) phases within both leaflets was obtained with palmitic acid as the anchoring group. In contrast, tethering of the PSM with oleic acid interfered with the phase separation in the surface-proximal leaflet. We exploited this feature for the assembly of l_o domains within PSMs into defined structures by binary micropatterning of palmitic and oleic acid into complementary areas. Ternary lipid mixtures spontaneously separated into l_o and l_d phases controlled by the geometry of the underlying tethers. Transmembrane proteins reconstituted in these phase-separated PSMs strictly partitioned into the l_d phase. Hence, the l_o phase could be used for confining transmembrane proteins into microscopic and submicroscopic domains.

Phase separation of lipid membranes into liquid-disordered (l_d) and liquid-ordered (l_o) domains has been recognized as a fundamental principle for the functional organization of proteins and lipids within the plasma membrane.[1−5] For the exploration of protein function in the context of a phase-separating lipid environment under controlled conditions in vitro, model systems mimicking the key features of plasma membrane domains are required.[6,7] For this purpose, giant unilamellar vesicles (GUVs) are frequently used as model systems.[8−10] Spontaneous phase separation of ternary lipid mixtures is observed in GUVs, yet the spatial organization of the phase-separated membranes is an entirely stochastic, time- and lipid-composition-dependent process that often leads to complete coalescence of the lipid phases. Moreover, proteins are difficult to reconstitute into GUVs, and few reports of transmembrane proteins reconstituted into phase-separated GUVs are available.[11] Polymer-supported membranes (PSMs) provide an elegant means for probing diffusion, interactions, and conformations of proteins in lipid bilayers with defined lipid composition.[12−15] Proteins are readily reconstituted into PSMs,[16−18] thus offering the potential to study transmembrane proteins in phase-separated membranes. PSMs have been demonstrated to allow the formation of registered l_o domains by Langmuir−Blodgett/Langmuir−Schaefer (LB/LS) deposition of preseparated lipid monolayers.[19] Microstructured assembly of phase-separating lipid membranes on solid supports to date has been achieved only by highly specialized approaches.[20−22]

PSMs are frequently based on hydrophobic tethering groups that are anchored into the surface-proximal leaflet of the membrane.[12,14] The density of the tethering groups has been shown to play a critical role in the diffusion of lipids and transmembrane proteins in tethered PSMs.[23] However, the possibilities for manipulating lipid phase separation by varying the structure of these tethering groups have not yet been explored.

In this work, we established an approach for spatial control of lipid phase separation in tethered PSMs on micropatterned supports. To this end, we employed spontaneous lipid phase separation on a poly(ethylene glycol) (PEG) polymer brush functionalized with palmitic acid (PA) (Figure 1a).[18] To obtain a phase-separating PSM, lipid vesicles were prepared from a ternary lipid mixture of 1,2-dioleoyl-*sn*-glycero-3-phosphocho-

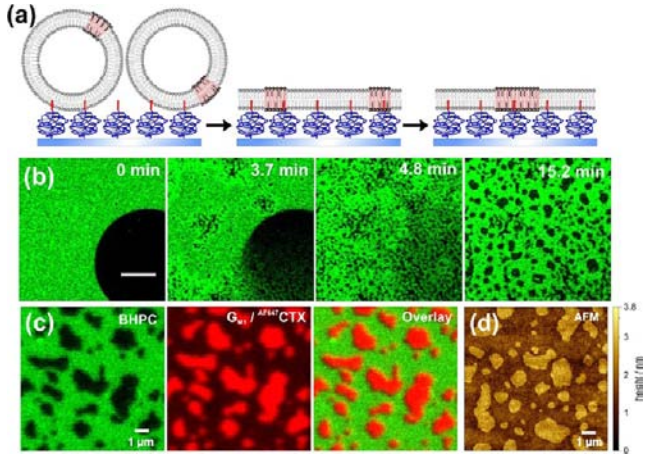

Figure 1. Lipid microdomain formation in a PSM. (a) Cartoon depicting vesicle capture and coalescence of submicroscopic lipid microdomains after induction of vesicle fusion. (b) Time-lapse fluorescence images capturing lipid phase separation after vesicle fusion was induced by addition of PEG solution. (c) Staining of the l_o and l_d domains by BHPC (green) and G_{M1}/^{AF647}CTX (red), respectively. (d) AFM image of a phase-separated membrane (in the absence of ^{AF647}CTX).

Received: October 15, 2012
Published: January 5, 2013

   dx.doi.org/10.1021/ja310186g | *J. Am. Chem. Soc.* 2013, 135, 1189−1192

line, sphingomyelin, and cholesterol doped with a fluorescent lipid analogue [β-BODIPY FL C5-hexadecylphosphocholine (BHPC) or 1′-dioctadecyl-3,3,3′,3′-tetramethylindodicarbocyanine 4-chlorobenzenesulfonate (DiD)] as a probe for l_d domains. These vesicles were captured on a PEG polymer brush on a glass substrate functionalized with PA moieties. After vesicle capture, a homogeneous fluorescence distribution was observed, and no fluorescence recovery after photobleaching (FRAP) of a circular spot occurred, confirming that surface-bound vesicles remained intact under these conditions (Figure 1b). After addition of a PEG solution to induce vesicle fusion, however, rapid formation of microscopic domains with substantially lower fluorescence intensities was observed [Figure 1b; also see video 1 in the Supporting Information (SI)], suggesting the formation of l_o domains in the fused lipid bilayer. Within the first minutes after microdomain formation, fusion into larger domains could be observed. After ~15 min, no further changes in the patterns were observed, which can be ascribed to the very low mobility of entire l_o domains due to tethering to the surface. In the photobleached area, the fluorescence fully recovered, corroborating the formation of a contiguous bilayer. This was further supported by the observation that elevating the temperature above the melting point of the l_o phase yielded homogeneous fluorescence with completely mobile lipids (Figure S1 in the SI).

The formation of l_o domains was further confirmed by studies of binding of cholera toxin subunit B labeled with Alexa Fluor 647 (^{AF647}CTX) to a PSM formed from a ternary lipid mixture containing 1% of the ganglioside G_{M1} as a marker for the l_o phase. Strong enrichment of ^{AF647}CTX in the domains excluding BHPC was observed (Figure 1c). The formation of l_o domains was further confirmed by atomic force microscopy (AFM) imaging of phase-separated membranes (Figure 1d). Microdomains whose height was increased by 1 nm relative to the surrounding membrane were observed, in good agreement with similar studies on mica-supported phase-separated membranes.[24] Single-molecule tracking was employed to characterize the diffusion of BHPC within the l_d and l_o domains, and diffusion constants (D) of 3.1 ± 0.5 and 0.38 ± 0.1 $\mu m^2/s$, respectively, were obtained (Figure S2), in good agreement with the literature.[25]

As a model transmembrane protein, maltose binding protein (MBP) fused to the transmembrane helix of the type-I interferon receptor subunit (IFNAR1) labeled with DY-649 (^{DY649}MBP-TM1) was reconstituted into a phase-separating PSM. Highly efficient exclusion of ^{DY649}MBP-TM1 from the l_o phase was observed (Figure S3), in line with the results of previous studies on transmembrane proteins in phase-separating model membranes.[26,27] Rapid diffusion of both lipid and transmembrane proteins within the l_d domains was confirmed by FRAP (Figure S3). However, an immobile fraction of fluorescent protein was always present in the l_o and l_d phases.

Palmitoylation has been shown to target proteins into ordered lipid domains.[28] Thus, PA was expected to allow or even promote l_o domain formation, as the density of PA moieties was relatively high (~0.5/nm^2).[18] Reducing the density of PA moieties, however, did not significantly alter the phase-separation properties (Figure S4).

We speculated that the formation of l_o domains could be controlled by the structure of the tethering moiety. To interfere with l_o domain formation, we coupled unsaturated oleic acid (OA) instead of saturated PA to the PEG polymer brush. Vesicle capture and fusion were possible on these surfaces with very similar efficacy, and the formation of lipid microdomains excluding the l_d marker was observed (Figure 2). However, the shape of these domains was characteristically different compared

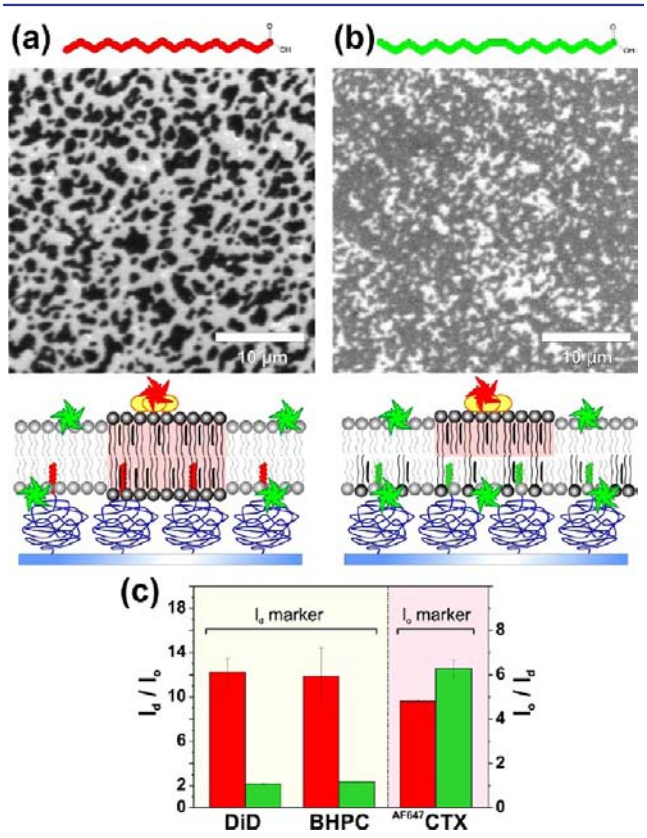

Figure 2. (a, b) Lipid phase separation in PSMs tethered by (a) PA and (b) OA. In the fluorescence images, DiD was used as a marker for the l_d phase. The cartoons depict the interpretation of the observed differences in the staining with different lipid-phase markers (green stars, DiD; red stars, ^{AF647}CTX). (c) Relative distributions of different lipid-phase markers between the apparent l_d and l_o phases observed for (red) PA- and (green) OA-tethered membranes. Left side: data for the l_d phase markers DiD and BHPC (l_d vs l_o). Right side: data for the l_o phase marker ^{AF647}CTX (l_o vs l_d), which can access only the surface-distal leaflet of the membrane.

with phase-separated PSMs tethered by PA, and the partitioning of the l_d marker was significantly less prominent. Quantitative analysis of the fluorescence intensity yielded ~50% intensity of the l_d marker in the microdomains of OA-tethered membranes (Figure 2c). We hypothesized that the tethering by OA moieties interferes with lipid phase separation in the surface-proximal leaflet, while phase separation is still possible in the surface-distal leaflet.

Indeed, ^{AF647}CTX binding to microdomains formed on OA-tethered PSMs was observed to occur with a similar partitioning constant as on PA-tethered PSMs (Figure 2c), confirming the formation of l_o domains in the surface-distal leaflet. The increased height within these regimes observed by AFM imaging further corroborated the formation of l_o domains in the surface-distal leaflet (Figure S5). Strikingly, the model transmembrane protein ^{DY649}MBP-TM1 was excluded from these as efficiently as from the trans-bilayer l_o domains obtained on PA-functionalized surfaces (Figure S6).

On the basis of the observation that OA interferes with trans-bilayer l_o domain formation, we anticipated that on micropatterned functionalized surfaces presenting PA and OA in

dx.doi.org/10.1021/ja310186g | J. Am. Chem. Soc. 2013, 135, 1189−1192

different areas, l_o phases would preferentially form in PA-tethered regions, allowing domain registration across the lipid bilayer (Figure 3a). To obtain such binary micropatterns, we used

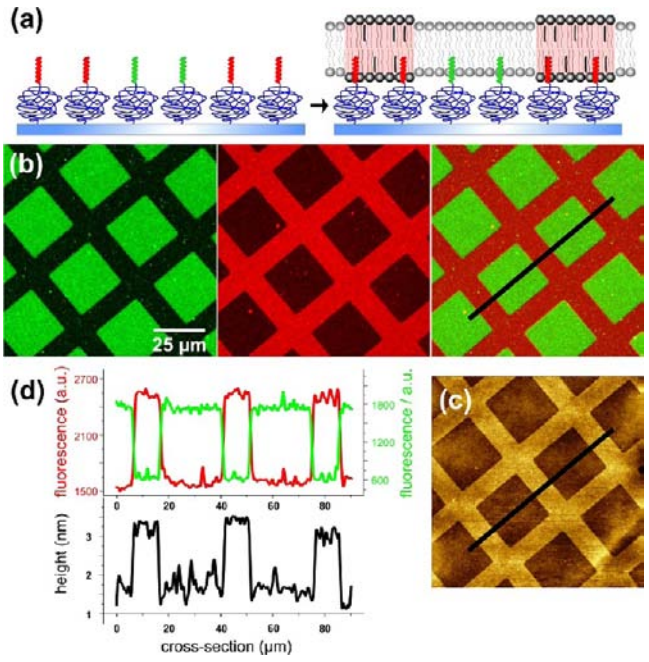

Figure 3. Spatial organization of lipid phases in PSMs on a micropatterned support. (a) Surfaces were functionalized with (red) PA and (green) OA in a spatially resolved manner in order to attract l_o phases selectively into areas functionalized with PA. (b) After fusion of vesicles comprising ternary lipid mixtures on theses surfaces, the l_d and l_o phases were imaged using BHPC (green) and G_{M1}/^{AF647}CTX (red), respectively, as probes. (c) AFM topography image of the phase-separated membrane loaded with CTX. (d) Intensity (top) and height (bottom) profiles along the black line indicated in (b) and (c).

nitroveratryloxycarbonyl (NVOC) groups to cage the amine groups of the PEG polymers coupled to the glass support[29] and then uncaged them by UV illumination through a photomask, followed by reaction with PA (Figure S7). Subsequently, remaining NVOC-protected amines were uncaged and reacted with OA. Strikingly, lipid phase separation into geometries defined by the PA/OA micropattern was observed when the l_d and l_o phases were stained with BHPC and ^{AF647}CTX, respectively, as well as by AFM imaging (Figure 3b–d).

The diffusion constants of the lipid probe within the micropatterned l_d and l_o domains as obtained by single-molecule tracking (D = 3.15 ± 0.3 and 0.36 ± 0.035 $\mu m^2/s$, respectively; Figure S8) were in good agreement with the values obtained for these domains on nonpatterned support. Moreover, we explored the kinetics of lipids and proteins crossing l_o domains by bleaching fluorescent probes inside l_d structures that were fully confined by l_o phase. FRAP in the confined domains was observed for BHPC (Figure 4), confirming partitioning and diffusion of this lipid analogue within the l_o domain. With increasing size of the l_o barrier (Figure S9), we observed slower recovery kinetics of BHPC (Figure 4), which was qualitatively in line with a simulation based on the experimentally determined diffusion and partitioning parameters (Figure S10 and video 2).

In contrast, no diffusion of the transmembrane protein ^{DY649}MBP-TM1 across the l_o barriers was detectable (Figure S11). When a segment within the l_d domain was photobleached,

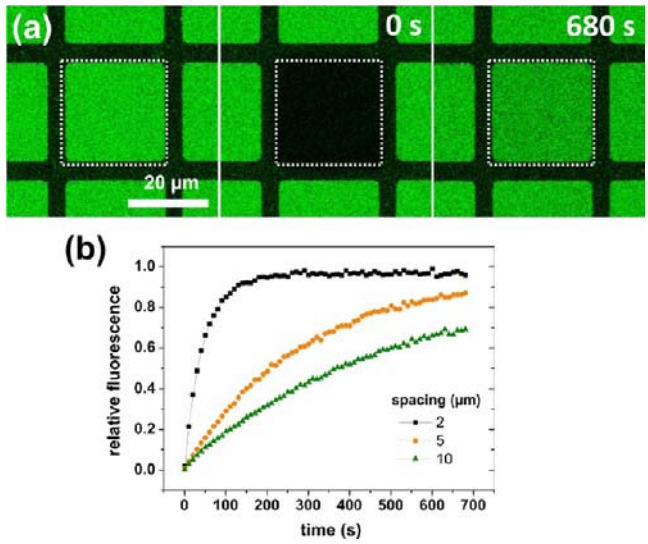

Figure 4. Lipid diffusion in micropatterned lipid phases. (a) Fluorescence recovery after full bleaching of BHPC in an l_d domain confined by an l_o phase barrier. The bleached area is indicated by the dotted line. (b) FRAP curves obtained for different widths of the confining l_o barrier.

free diffusion of the protein within the l_d phase was confirmed (Figure 5). However, no significant recovery of the fluorescence within the total l_d domain was observed, confirming that the mobile transmembrane protein was fully excluded from the l_o phase.

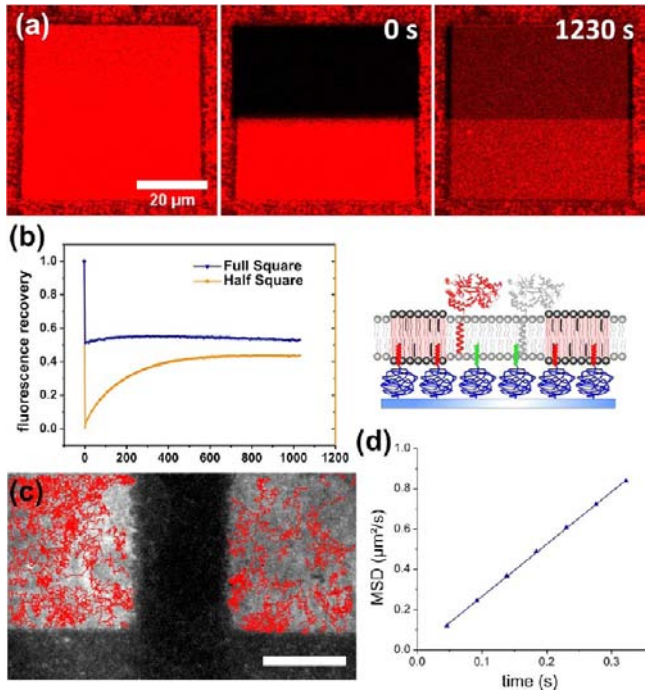

Figure 5. Protein diffusion in micropatterned lipid phases. (a) FRAP of ^{DY649}MBP-TM1 in a segment of an l_d domain confined by an l_o phase barrier. (b) FRAP curves of the bleached segment (orange) and the entire confined l_d phase (blue). (c) Trajectories of individual ^{DY649}MBP-TM1 molecules diffusing within the l_d domain (scale bar: 10 μm). (d) Mean-square displacement analysis of ^{DY649}MBP-TM1 diffusion within the l_d domain.

dx.doi.org/10.1021/ja310186g | J. Am. Chem. Soc. 2013, 135, 1189–1192

This was further confirmed by single-molecule tracking experiments, which revealed rapid diffusion of ^{DY649}MBP-TM1 ($D = 0.61 \pm 0.05\ \mu m^2/s$) as well as the impermeability of the surrounding l_o phases (Figure 5c,d and video 3). Thus, micropatterned l_o phases within PSMs can be employed as semipermeable membrane segments for confining the diffusion of lipids and proteins into microdomains.

These results clearly establish that lipid phase separation in tethered PSMs can be controlled by the properties of the tethering moieties. Suitable artificial model systems are key for a quantitative understanding of the principles underlying the submicroscopic organization of the plasma membrane. However, current systems based on spontaneous lipid phase separation show fundamental differences relative to the cellular situation.[30] The key shortcomings of model membrane rafts are their large sizes and low permeabilities for membrane proteins.[27] Here we have demonstrated the feasibility of spatially organizing phase-separated lipid membranes on solid supports. As expected, membrane tethering by PA supported the formation of lipid phases, while OA strongly interfered with l_o phase formation in the surface-proximal leaflet. The preferential l_o phase formation in PA-tethered regimes within binary PA/OA micropatterns is probably due to the energetically favored trans-bilayer registration of l_o domains. These findings support the currently emerging hypothesis that anchoring of the membrane to the cortical cytoskeleton by lipids and proteins plays an important role in regulating the formation of small and highly dynamic membrane rafts.[4,31−33] Our results experimentally confirm that such membrane anchors can interfere with the coalescence of membrane rafts into larger entities, as suggested by simulations.[34,35]

While l_o domain micropatterning has previously been achieved in solid-supported membranes,[36,37] here we for the first time established this possibility for polymer-supported membranes, which allow functional reconstitution of transmembrane proteins. Control of lipid phase separation in such tethered membranes opens exciting new possibilities for mimicking plasma membrane microdomain formation. The properties of proteins and lipids in the context of phase-separating lipid membranes can be studied more systematically by applying well-defined lipid phase geometries. Application of nanopatterning techniques will provide submicroscopic l_o domains for mimicking the small and more dynamic nature of membrane rafts. Moreover, systematic manipulation of the formation and properties of l_o and l_d domains will be possible by using different transmembrane tethers, including proteins. Combining these efforts may provide a basis for exploring the dynamic partitioning of membrane proteins into plasma membrane rafts in a quantitative manner.

■ ASSOCIATED CONTENT

Supporting Information

Detailed experimental procedures, supporting figures, and videos (AVI). This material is available free of charge via the Internet at http://pubs.acs.org.

■ AUTHOR INFORMATION

Corresponding Author

Piehler@uos.de

Notes

The authors declare no competing financial interest.

■ ACKNOWLEDGMENTS

This project was supported by the DFG (PI405-4 and SFB 944) and the European Community's Seventh Framework Programme (FP7/2007−2013) under Grant Agreement 223608 (IFNaction). We thank G. Hikade and H. Kenneweg for excellent technical support and C. P. Richter for help with data evaluation.

■ REFERENCES

(1) Lingwood, D.; Simons, K. *Science* **2010**, *327*, 46.
(2) Lingwood, D.; Kaiser, H. J.; Levental, I.; Simons, K. *Biochem. Soc. Trans.* **2009**, *37*, 955.
(3) Simons, K.; Toomre, D. *Nat. Rev. Mol. Cell Biol.* **2000**, *1*, 31.
(4) Kusumi, A.; Fujiwara, T. K.; Morone, N.; Yoshida, K. J.; Chadda, R.; Xie, M.; Kasai, R. S.; Suzuki, K. G. *Semin. Cell Dev. Biol.* **2012**, *23*, 126.
(5) Kusumi, A.; Shirai, Y. M.; Koyama-Honda, I.; Suzuki, K. G. N.; Fujiwara, T. K. *FEBS Lett.* **2010**, *584*, 1814.
(6) Kaiser, H. J.; Lingwood, D.; Levental, I.; Sampaio, J. L.; Kalvodova, L.; Rajendran, L.; Simons, K. *Proc. Natl. Acad. Sci. U.S.A.* **2009**, *106*, 16645.
(7) Loose, M.; Schwille, P. *J. Struct. Biol.* **2009**, *168*, 143.
(8) Kahya, N.; Scherfeld, D.; Bacia, K.; Schwille, P. *J. Struct. Biol.* **2004**, *147*, 77.
(9) Sezgin, E.; Levental, I.; Grzybek, M.; Schwarzmann, G.; Mueller, V.; Honigmann, A.; Belov, V. N.; Eggeling, C.; Coskun, U.; Simons, K.; Schwille, P. *Biochim. Biophys. Acta* **2012**, *1818*, 1777.
(10) Kahya, N. *Biochim. Biophys. Acta* **2010**, *1798*, 1392.
(11) Fenz, S. F.; Sengupta, K. *Integr. Biol.* **2012**, *4*, 982.
(12) Tanaka, M.; Sackmann, E. *Nature* **2005**, *437*, 656.
(13) Sackmann, E.; Tanaka, M. *Trends Biotechnol.* **2000**, *18*, 58.
(14) Sinner, E. K.; Ritz, S.; Naumann, R.; Schiller, S.; Knoll, W. *Adv. Clin. Chem.* **2009**, *49*, 159.
(15) Sinner, E. K.; Knoll, W. *Curr. Opin. Chem. Biol.* **2001**, *5*, 705.
(16) Wagner, M. L.; Tamm, L. K. *Biophys. J.* **2001**, *81*, 266.
(17) Wagner, M. L.; Tamm, L. K. *Biophys. J.* **2000**, *79*, 1400.
(18) Roder, F.; Waichman, S.; Paterok, D.; Schubert, R.; Richter, C.; Liedberg, B.; Piehler, J. *Anal. Chem.* **2011**, *83*, 6792.
(19) Garg, S.; Ruhe, J.; Ludtke, K.; Jordan, R.; Naumann, C. A. *Biophys. J.* **2007**, *92*, 1263.
(20) Lee, B. K.; Lee, H. Y.; Kim, P.; Suh, K. Y.; Kawai, T. *Lab Chip* **2009**, *9*, 132.
(21) Orth, A.; Johannes, L.; Romer, W.; Steinem, C. *ChemPhysChem* **2012**, *13*, 108.
(22) Chao, L.; Daniel, S. *J. Am. Chem. Soc.* **2011**, *133*, 15635.
(23) Deverall, M. A.; Gindl, E.; Sinner, E. K.; Besir, H.; Ruehe, J.; Saxton, M. J.; Naumann, C. A. *Biophys. J.* **2005**, *88*, 1875.
(24) Yuan, C.; Furlong, J.; Burgos, P.; Johnston, L. J. *Biophys. J.* **2002**, *82*, 2526.
(25) Ries, J.; Chiantia, S.; Schwille, P. *Biophys. J.* **2009**, *96*, 1999.
(26) Bacia, K.; Schuette, C. G.; Kahya, N.; Jahn, R.; Schwille, P. *J. Biol. Chem.* **2004**, *279*, 37951.
(27) Nikolaus, J.; Scolari, S.; Bayraktarov, E.; Jungnick, N.; Engel, S.; Pia Plazzo, A.; Stockl, M.; Volkmer, R.; Veit, M.; Herrmann, A. *Biophys. J.* **2010**, *99*, 489.
(28) Levental, I.; Grzybek, M.; Simons, K. *Biochemistry* **2010**, *49*, 6305.
(29) Waichman, S.; Bhagawati, M.; Podoplelova, Y.; Reichel, A.; Brunk, A.; Paterok, D.; Piehler, J. *Anal. Chem.* **2010**, *82*, 1478.
(30) London, E. *Biochim. Biophys. Acta* **2005**, *1746*, 203.
(31) Viola, A.; Gupta, N. *Nat. Rev. Immunol.* **2007**, *7*, 889.
(32) Chichili, G. R.; Rodgers, W. *Cell. Mol. Life Sci.* **2009**, *66*, 2319.
(33) Liu, A. P.; Fletcher, D. A. *Biophys. J.* **2006**, *91*, 4064.
(34) Ehrig, J.; Petrov, E. P.; Schwille, P. *Biophys. J.* **2011**, *100*, 80.
(35) Machta, B. B.; Papanikolaou, S.; Sethna, J. P.; Veatch, S. L. *Biophys. J.* **2011**, *100*, 1668.
(36) Yoon, T. Y.; Jeong, C.; Lee, S. W.; Kim, J. H.; Choi, M. C.; Kim, S. J.; Kim, M. W.; Lee, S. D. *Nat. Mater.* **2006**, *5*, 281.
(37) Okazaki, T.; Tatsu, Y.; Morigaki, K. *Langmuir* **2010**, *26*, 4126.